Dalton Transactions

High Catalytic Methane Oxidation Activity of Monocationic □-Nitrido-Bridged Iron Phthalocyanine Dimer with Sixteen Peripheral Methyl Groups

Journal:	*Dalton Transactions*
Manuscript ID	DT-ART-03-2021-000941.R1
Article Type:	Paper
Date Submitted by the Author:	14-Apr-2021
Complete List of Authors:	Yamada, Yasuyuki; Nagoya University, Research Center for Materials Science Kura, Jyunichi; Nagoya University, Department of Chemistry Toyoda, Yuka; Nagoya University, Department of Chemistry Tanaka, Kentaro; Nagoya University, Department of Chemistry, Graduate School of Science

PAPER

High Catalytic Methane Oxidation Activity of Monocationic μ–Nitrido-Bridged Iron Phthalocyanine Dimer with Sixteen Methyl Groups

Received 00th January 20xx,
Accepted 00th January 20xx

DOI: 10.1039/x0xx00000x

Yasuyuki Yamada,*[a,b,c] Jyunichi Kura,[a] Yuka Toyoda,[b] and Kentaro Tanaka *[a]

Herein, we report the highly potent catalytic methane oxidation activity of a monocationic μ-nitrido-bridged iron phthalocyanine dimer with 16 peripheral methyl groups. It was confirmed that this complex oxidized methane stably into MeOH, HCHO, and HCOOH in a catalytic manner in an acidic aqueous solution containing excess H_2O_2 at 60 °C. The total turnover number of the reaction reached 135 after 12 h, which is almost seven times higher than that of a monocatinoic μ-nitrido-bridged iron phthalocyanine dimer with no peripheral substituents. This suggests that the increased number of peripheral electron-donating substituents could have facilitated the generation of a reactive high-valent iron-oxo species as well as hydrogen abstraction from methane by the reactive iron-oxo species.

Introduction

Methane has long been expected to be a next-generation carbon resource because it is abundant in nature as natural gas and methane hydrates.[1,2] However, methane has such a high C-H bond dissociation energy (104.9 kcal/mol) among a variety of organic compounds that direct and low-temperature conversion of methane into more valuable raw chemicals such as MeOH is an exceedingly difficult conversion that necessitates catalysis.[3,4] Therefore, the development of novel catalysts that can convert methane efficiently under mild reaction conditions is strongly desired.[5-18]

Methane monooxygenase (MMO), a kind of natural oxygenase, is known to efficiently convert methane into MeOH under mild conditions.[19,20] The fact that some MMOs utilize high-valent iron-oxo species as the reactive center has led a number of researchers to develop a variety of biomimetic iron-oxo-based oxidation catalysts.[21–25] Molecular catalysts have a remarkable advantage in that their catalytic properties can be designed and fine-tuned by synthetic modification. For example, it is known that the generation rate and reactivity of high-valent iron oxo species of a monomeric iron porphyrin can be controlled by peripheral substituents.[26–28] Although these challenges have led to great success in investigating the reaction mechanism of the high-valent iron-oxo species, only a few of them can actually activate the C-H bond of methane at lower temperatures below than 100 °C until now.[13-17]

The μ-nitrido-bridged iron phthalocyanine dimer is one of the most potent methane oxidation catalysts reported to date. Sorokin et al. found that the treatment of the μ-nitrido-bridged iron phthalocyanine dimer **1** or its 1e⁻-oxidized monocationic species **1**⁺

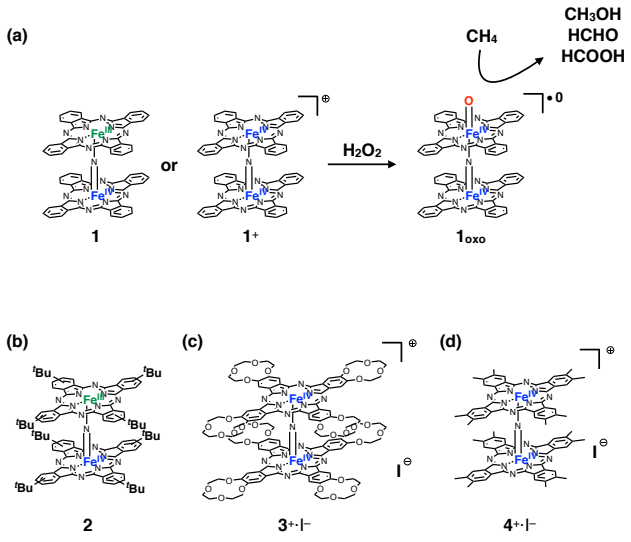

Figure 1 (a) Formation of high-valent iron oxo species $\mathbf{1_{oxo}}$ from **1** or **1**⁺. $\mathbf{1_{oxo}}$ shows methane oxidation activity. Structures of (b) μ-nitrido-bridged iron phthalocyanine dimer bearing eight *tert*-butyl groups (**2**), (c) monocationic μ-nitrido-bridged iron phthalocyanine dimer with eight peripheral 12-crown-4 units (**3**⁺), and (d) monocationic μ-nitrido-bridged iron phthalocyanine dimer with sixteen methyl groups (**4**⁺).

[a] *Department of Chemistry, Graduate School of Science, Nagoya University, Furo-cho, Chikusa-ku, Nagoya 464-8602, Japan.*
[b] *Research Center for Materials Science, Nagoya University, Furo-cho, Chikusa-ku, Nagoya 464-8602, Japan.*
[c] *JST, PRESTO, 4-1-8 Honcho, Kawaguchi, Saitama, 332-0012, Japan.*
†*E-mail*: yy@chem.nagoya-u.ac.jp, kentaro@chem.nagoya-u.ac.jp
Electronic Supplementary Information (ESI) available: [details of any supplementary information available should be included here]. See DOI: 10.1039/x0xx00000x

with H_2O_2 in an acidic aqueous solution produced the high-valent iron-oxo species $\mathbf{1}_{oxo}$, which acted as a reactive species for methane oxidation (Figure 1a).[13-16] Until now, **1** (**1**$^+$), $\mathbf{1}_{oxo}$, and their related compounds were investigated by using EPR, absorption, Mössbauer, Mass, XANES, and EXAFS spectroscopies *etc.* in order to understand the electronic structures and reactivities of these complexes.[13–16,29–32] Theoretical calculations were also performed by several groups, revealing the superiority of the μ-nitrido-bridged dinulcear iron structure for achieving strong methane oxidation activity.[33–36] Calculation by de Visser et al. also suggested that the origin of the high reactivity of $\mathbf{1}_{oxo}$ is related to the orbital mixing pattern along with the Fe=N-Fe=O axis, where the axial FePc=N- moiety (Pc represents phthalocyanine) donates sufficient electron density to FePc=O to affect the basicity of the terminal oxygen as well as the strength of the O-H bond of the iron-hydroxo complex formed during the methane oxidation.[34]

In the course of pursuing higher catalytic methane oxidation activity, Sorokin et al. reported that the methane oxidation activity of **1** was affected by the substituents introduced onto the phthalocyanine ring.[16] The activity was almost doubled when eight electron-donating *tert*-butyl moieties were introduced (**2** in Figure 1b), but decreased when eight electron-withdrawing sulfonyl groups were introduced. This suggests that the introduction of larger numbers of electron-donating substituents at the periphery of the phthalocyanine ring might help to achieve higher catalytic methane oxidation activity. However, to the best of our knowledge, there are no other reports on the stable catalytic methane oxidation activity of μ-nitride-bridged iron phthalocyanine dimers with electron-donating substituents other than **2**.

In our previous research, we synthesized a μ-nitrido-bridged iron phthalocyanine dimer bearing eight 12-crown-4 unis (**3**$^+$·I$^-$), as shown in Figure 1c.[37] We expected **3**$^+$·I$^-$ to show high catalytic methane oxidation activity. However, it decomposed in an acidic aqueous solution containing H_2O_2 at 60 °C, although the decomposed compound showed Fenton-type methane oxidation activity. It is possible that the introduction of alkoxy moieties on the periphery of phthalocyanine ring destabilized the iron-oxo species generated *in situ*. Therefore, we decided to introduce methyl groups instead of 12-crown-4 units because the Hammett substituent constant of the methyl group (σ_p = –0.17) is almost comparable to those of the *tert*-butyl group (σ_p = –0.20) and the methoxy group (σ_p = –0.27).[38] In this study, we synthesized a novel μ-nitrido-bridged iron phthalocyanine dimer with 16 methyl groups on the phthalocyanine units (**4**$^+$·I$^-$ in Figure 1d) and investigated its catalytic methane oxidation activity.

Results and Discussion

The synthesis of **4**$^+$·I$^-$ is shown in Figure 2a. An iron phthalocyanine with eight methyl moieties (**6**) was obtained by thermal tetramerization of the 4,5-dimethylphthalonitrile **5** in ethylene glycol in the presence of $Fe(CO)_5$. Heating a mixture of **6** and NaN_3 in 1-chloronaphthalene at 190 °C gave the neutral species of μ-nitride-bridged iron phthalocyanine dimer **4**. As **4** was gradually oxidized in the air, it was converted into its 1e$^-$-oxidized monocationic species **4**$^+$·I$^-$ by oxidation with I_2 without purification. Although **4**$^+$·I$^-$ showed poor solubility in many common organic solvents, which made purification by column chromatography or recrystallization difficult, fortuitously, the solubility of **4**$^+$·I$^-$ improved when pyridine was used as a solvent and this allowed us to purify the product. This is presumably because pyridine coordinated to the iron center and prevented the formation of the stacked aggregate of **4**$^+$.[39,40]

The MALDI-TOF-MS spectrum of **4**$^+$·I$^-$ showed signals at around *m/z* = 1374, which was in good agreement with the signals in the calculated isotopic distribution pattern of **4**$^+$ as depicted in Figure S3 in the Supporting Information. The ^{1}H-NMR spectrum of **4**$^+$·I$^-$ showed signals at 9.21 ppm and 3.23 ppm (Figure 2b), which corresponded to the alpha proton of the phthalocyanine ring and

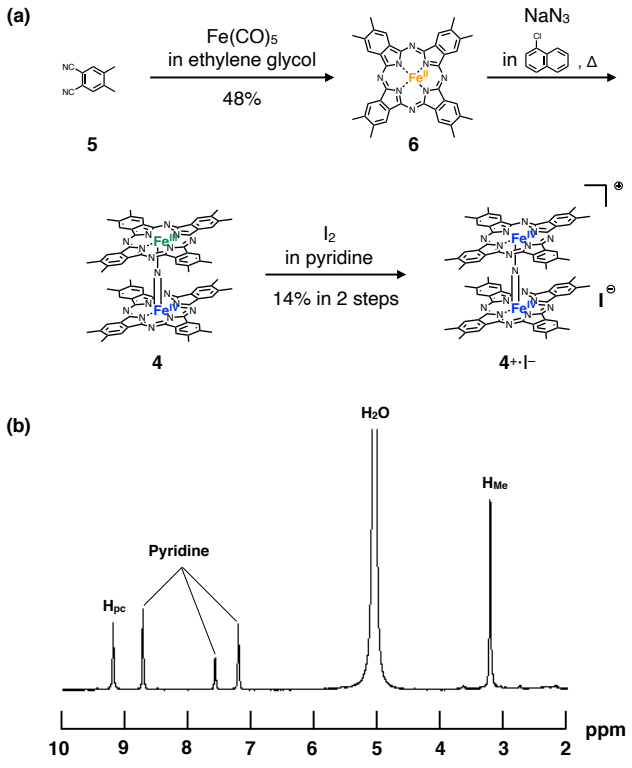

Figure 2 (a) Synthesis of **2**$^+$·I$^-$. (b) ^{1}H-NMR spectrum of **2**$^+$·I$^-$ in pyridine-d_5.

the methyl group protons, respectively. Both of these signals were observed as singlets, suggesting that the upper and lower phthalocyanine rings are equivalent in pyridine. The neutral μ-nitrido-bridged iron tetraphenylporphyrin dimer that includes a Fe(III) and a Fe(IV) centers has been reported to exhibit a significant broadening of ^{1}H-NMR signals, whereas its 1e$^-$-oxidized monocationic species, which possesses two Fe(IV) centers, shows sharp ^{1}H-NMR signals.[41–43] This suggests that the two Fe(IV) centers interact antiferromagnetically in a monocationic species.[37,39,44] As **4**$^+$·I$^-$ showed sharp ^{1}H-NMR signals, we concluded that **4**$^+$·I$^-$ also possesses two Fe(IV) centers.

(a)

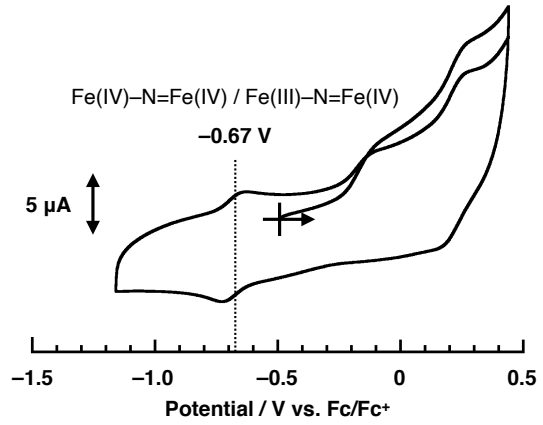

(b)

Complex	$E^{\circ\prime}$ (Fe(IV)-N=Fe(IV) / Fe(III)-N=Fe(IV))	Hammett Substituent Constant σ_p (Substituent)
1$^{+\cdot}$I$^-$	–0.58	0.00 (-H)
3$^{+\cdot}$I$^-$	–0.66	–0.27 (-OCH$_3$)[a]
4$^{+\cdot}$I$^-$	–0.67	–0.17 (-CH$_3$)

Figure 3 (a) Cyclic voltammogram of **4**$^{+\cdot}$I$^-$ (200 μM) in a pyridine solution containing 100 mM of ^{n}Bu$_4$N$^+$·PF$_6^-$ at room temperature. [Scan rate] = 400 mV/s. (b) Comparison of the redox potentials (V vs. Fc/Fc$^+$) of 1e$^-$ redox wave corresponding to Fe(IV)–N=Fe(IV)/Fe(III)–N=Fe(IV) of **1**$^{+\cdot}$I$^-$ (ref. 39), **3**$^{+\cdot}$I$^-$ (ref. 37), and **4**$^{+\cdot}$I$^-$. [a] Hammett substituent constant (σ_p) of methoxy group (-OCH$_3$) was shown for that of **3**$^{+\cdot}$I$^-$.

Figure 3a shows the cyclic voltammogram of **4**$^{+\cdot}$I$^-$ in pyridine containing 100 mM ^{n}Bu$_4$N$^+$·PF$_6^-$. One quasi-reversible 1e$^-$-redox wave and two irreversible oxidation waves were observed in the potential range of –1.2 V to +1.0 V vs. Fc/Fc$^+$. The redox wave at –0.67 V corresponded to the 1e$^-$ reduction of the iron center of **4**$^+$ (Fe(IV)-N=Fe(IV)/Fe(III)-N=Fe(IV)),[45] which showed significant negative shifts compared to that of the μ-nitrido-bridged iron phthalocyanine dimer with no peripheral substituent (Figure 3b). The degree of this negative shift of the redox wave ($\Delta E^{\circ\prime}$ = –0.09 V) is almost identical to that of the μ-nitrido-bridged iron phthalocyanine dimer bearing eight 12-crown-4 units ($\Delta E^{\circ\prime}$ = –0.08 V).[37,39] Considering the difference in the Hammett substituent constant shown in the Table in Figure 3b, this observation confirms the electron-donating character of the methyl groups introduced on the phthalocyanine units.

Encouraged by these observations, we used **4**$^{+\cdot}$I$^-$ for the methane oxidation reaction. The merit of using the monocationic species **4**$^+$ instead of the neutral species **4** is that **4**$^+$ is stable against oxidation by air. H_2O was used as the solvent because it is comparatively stable against the oxidation by the high-valent iron-oxo species. However, the catalyst molecules were insoluble in H_2O. Therefore, we carried out the reaction by using silica gel-supported catalysts on which **4**$^{+\cdot}$I$^-$ was adsorbed. The methane oxidation reaction was performed at 60°C in an acidic aqueous solution in the presence of an excess amount of hydrogen peroxide under a methane atmosphere of 1.0 MPa. GC-MS analysis revealed the formation of the oxidized compounds of methane, namely MeOH, HCHO, and HCOOH, were observed as shown in Figure 4b and Table S1, suggesting that methane was oxidized according to the scheme shown in Figure 4a. The amounts of these oxidized products were significantly smaller in the absence of methane (under 1.0 M Pa of N_2), indicating that methane was indeed oxidized under these reaction conditions. The oxidized compounds observed in the absence of methane were presumably derived from the organic solvents adsorbed on the silica surface. It should also be mentioned

(a)

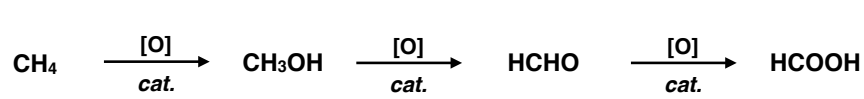

(b)

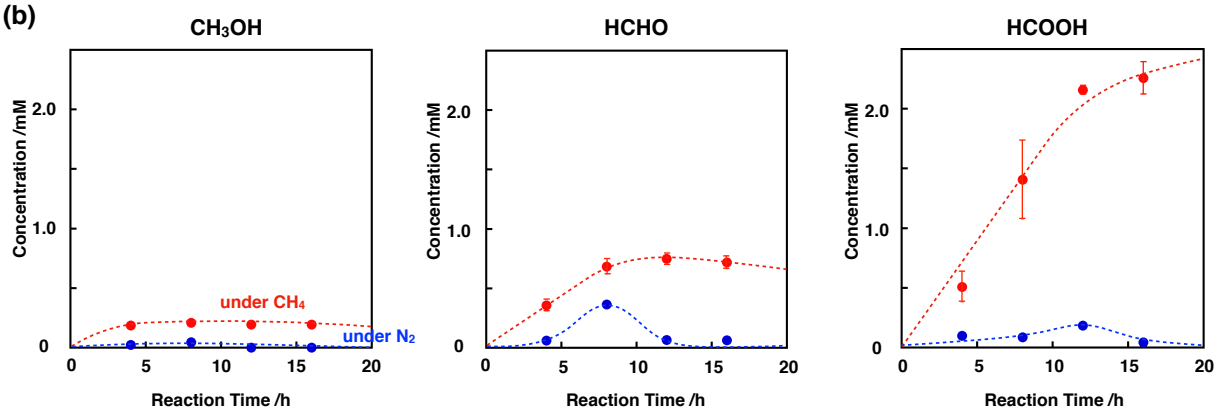

Figure 4 (a) Stepwise methane oxidation reaction. (b) Time dependence of concentrations of each oxidized product (MeOH, HCHO, and HCOOH) observed in the reaction in the presence of 1.0 MPa of methane (red closed circle) or in the absence of methane (under 1.0 MPa of N_2, blue closed circle) in an aqueous solution (3.0 mL) containing **4**$^{+\cdot}$I$^-$/SiO$_2$ (55 μM as **4**$^{+\cdot}$I$^-$), H_2O_2 (189 mM), and TFA (51 mM) at 60 °C. Error bars indicate standard deviations of three independent methane oxidation reactions.

that no apparent bleaching of the catalyst was not observed, which is in clear contrast to the significant bleaching of $\mathbf{3}^{+}\cdot I^{-}$ under the same reaction conditions (Figure S4).[37] Generally, significant bleaching of the catalyst is observed in the case of the Fenton type reaction where •OH acts as a reactive intermediate. Considering that the reaction was hardly quenched in the presence of the radical scavenger, Na_2SO_3 (Table S1, Entries 9 and 10 in the Supporting Information),[9] it is reasonable to conclude that the reaction was proceeded through the high-valent iron-oxo species of **4**, as in the case of **1** or **2**.

To evaluate the catalytic activity of $\mathbf{4}^{+}\cdot I^{-}/SiO_2$, we defined the effective total turnover number (TTN_{eff}) and effective methane conversion number (MCN_{eff}) according to equations (i)–(iv) based on the rationale that methane is oxidized in a stepwise manner (Figure 4a). MCN_{eff} is useful for evaluating the activity in the C-H activation of methane, whereas TTN_{eff} reflects the activity against the C-H activation of methane, MeOH, and HCHO.

$$TTN_{eff} = TTN_{(CH4)} - TTN_{(N2)} \quad \text{(i)}$$

$$TTN_{(CH4)} \text{ or } TTN_{(N2)} = (C_{MeOH} + 2 \times C_{HCHO} + 3 \times C_{HCOOH}) / C_{Cat} \quad \text{(ii)}$$

$$MCN_{eff} = MCN_{(CH4)} - MCN_{(N2)} \quad \text{(iii)}$$

$$MCN_{(CH4)} \text{ or } MCN_{(N2)} = (C_{MeOH} + C_{HCHO} + C_{HCOOH}) / C_{Cat} \quad \text{(iv)}$$

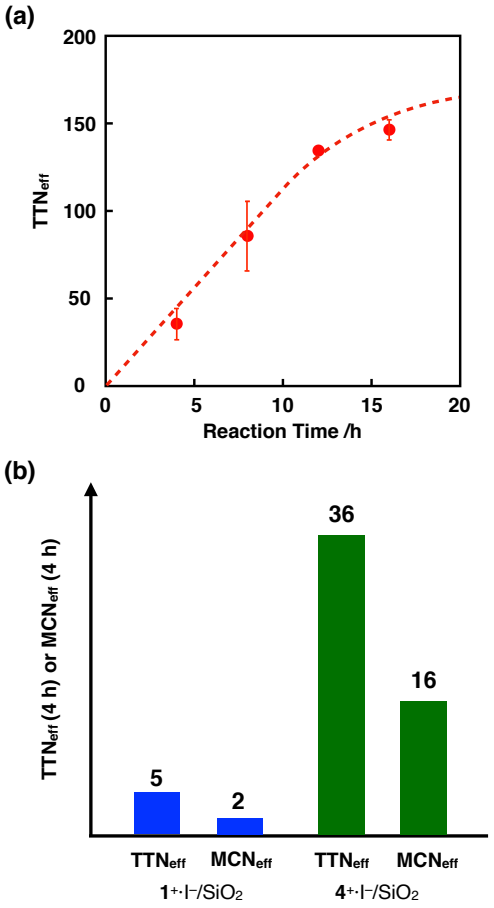

Figure 5 (a) Change in TTN_{eff} for the methane oxidation reaction by $\mathbf{4}^{+}\cdot I^{-}/SiO_2$. Error bars indicate standard deviation of three independent methane oxidation reactions. (b) Comparison of TTN_{eff} and MCN_{eff} for the methane oxidation reactions for 4 h by $\mathbf{1}^{+}\cdot I^{-}$ and $\mathbf{4}^{+}\cdot I^{-}$.

The time dependence of the TTN_{eff} is shown in Figure 5a. TTN_{eff} was increased almost linearly in the initial 12 h, suggesting this catalyst was stable under these reaction conditions. This observation is also different from the methane oxidation by $\mathbf{3}^{+}\cdot I^{-}/SiO_2$ under the same reaction conditions, where TTN_{eff} was almost negligible initially and gradually increased after 2 h.[37] The gradual decrease in TTN_{eff} of $\mathbf{4}^{+}\cdot I^{-}/SiO_2$ after 8 h can be attributed to the decrease in the concentration of H_2O_2 by the catalase reaction[46] and also to the overoxidation of HCOOH because of the high reactivity of the iron-oxo species of $\mathbf{4}^{+}$. It was confirmed that HCOOH was gradually oxidized under the same reaction conditions (Figure S5) because of the strong oxidizing activity of the oxo species of $\mathbf{4}^{+}$.

Figure 5b shows the comparison of TTN_{eff} and MCN_{eff} of $\mathbf{4}^{+}\cdot I^{-}/SiO_2$ after 4 h with those of $\mathbf{1}^{+}\cdot I^{-}/SiO_2$. Both TTN_{eff} and MCN_{eff} of the reaction with $\mathbf{4}^{+}\cdot I^{-}/SiO_2$ were significantly higher than those of the reaction with $\mathbf{1}^{+}\cdot I^{-}/SiO_2$. The TTN of a μ-nitrido-bridged iron phthalocyanine dimer bearing eight *tert*-butyl units **2** was reportedly as almost twice as that of **1** under similar reaction conditions.[16] Considering that both of the catalysts ($\mathbf{4}^{+}\cdot I^{-}/SiO_2$ and $\mathbf{1}^{+}\cdot I^{-}/SiO_2$) were stable without any apparent bleaching under these reaction conditions,[14,16] the higher degree of enhancement is presumably due to the increased number of electron-donating substituents introduced on the periphery of the phthalocyanine unit of the catalyst center of $\mathbf{4}^{+}$.

The proposed reaction mechanism and possible elucidation of the contribution of electron-donating methyl groups to the high methane oxidation activity of $\mathbf{4}^{+}\cdot I^{-}$ are summarized in Figure 6. The reactive intermediate is considered to be a high-valent iron-oxo species generated *in situ*.[13,15] It is generally considered that methane oxidation by high-valent iron oxo species undergoes a proton coupled electron transfer (PCET) mechanism, in which H atom abstraction and $1e^{-}$ oxidation proceed in a concerted manner.[47,48] Based on calculation, Sorokin and de Visser proposed that the introduction of electron-donating substituents is advantageous for H atom abstraction.[16] This can also be understood

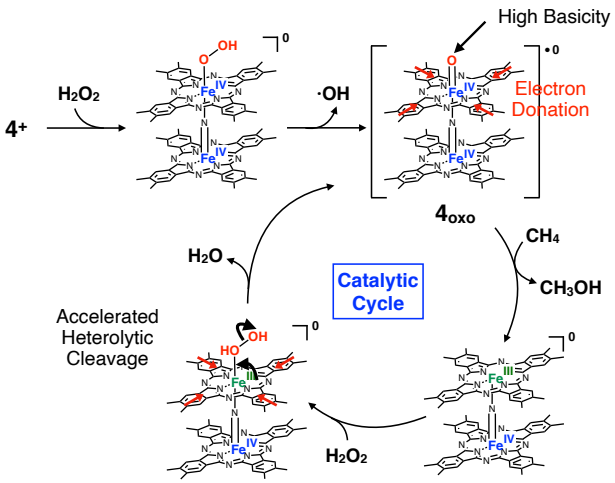

Figure 6 Proposed reaction mechanism and possible elucidation for the contribution of electron-donating methyl groups to the high methane oxidation activity of $\mathbf{4}^{+}$.

as electron-donating substituents increasing the basicity of the oxo species. On the strength of their experimental results, Sorokin and de Visser also suggested that the introduction of electron-donating substituents is beneficial for the formation of high-valent iron-oxo species,[16] and yet another possibility is that heterolytic cleavage of the O-O bonding of hydroperoxo species to produce the high-valent iron-oxo species is facilitated by electron-donating substituents.[28] Although the introduction of electron-donating substituents might be detrimental to achieving a more positive oxidation potential of the oxo species for efficient electron transfer from methane to the catalyst, the actual increase in the catalytic activity of **4** having 16 electron-donating groups may be explained by the predominating effect of increased basicity and production rate of the oxo species in this case.

As for a μ-nitrido-bridged iron porphyrin dimer that also shows high methane oxidation activity, DFT calculation by Phung and Pierloot suggested that the low-lying mixed valence excited state of the complex, O=Fe(V)-N=Fe(IV), might be essential for high reactivity.[36] In order to address the question how the peripheral electron-donating substituents of a μ-nitrido-bridged iron phthalocyanine dimer affect on the mixed-valence excited state, further research should be conducted.

Conclusions

In this study, we synthesized a novel μ-nitrido-bridged iron phthalocyanine dimers with 16 peripheral electron-donating methyl groups on the phthalocyanine moieties **4**$^{+}$·I^{-} and investigated its catalytic methane oxidation activity in an acidic aqueous solution containing excess H_2O_2. In contrast to the decomposition of the μ-nitrido-bridged iron phthalocyanine dimer bearing eight 12-crown-4 units (**3**$^{+}$·I^{-}) under the same reaction conditions, **4**$^{+}$·I^{-} was stable and catalyzed the conversion of methane into MeOH, HCHO, and HCOOH in a catalytic manner. It was found that **4**$^{+}$·I^{-} showed one of the most potent methane oxidation activities among a variety of molecular methane oxidation catalysts. We expect that these results will provide valuable information for designing more potent methane oxidation molecular catalysts based on μ-nitrido-bridged iron porphyrinoid dimers.

Experimental

General All reagents and solvents were purchased at the highest commercial quality available and used without further purification, unless otherwise stated. Monocationic μ-nitrido-bridged iron phthalocyanine dimers (**1**$^{+}$·I^{-}) was prepared according to our previous report.[39] ^{1}H NMR spectra were recorded on a JEOL JNM-ECS400-A (400 MHz for ^{1}H) spectrometer at a constant temperature of 298 K. Elemental analysis was performed on a Yanaco MT-6 analyzer. The absorption spectrum was recorded with a Hitachi U-4100 spectrophotometer in pyridine solutions at 20 ± 0.1 °C in 1.0 cm quartz cells. MALDI-TOF MS was performed on Bruker Daltonics ultraXtreme using α-CHCA as a matrix.

Synthesis of 1,2-dicyano-4,5-dimethylbenzene 5. 1,2-dibromo-4,5-dimethylbenzene (2.0 g, 7.7 mmol), CuCN (2.9 g, 32 mmol), and dry DMF (90 mL) were added to a 100 mL schlenk flask. Oxygen was removed by freezing-thaw method by 4 times. The suspension was stirred at 160 °C for 87 hrs, and then poured into 28% aqueous NH_3 (200 mL). After stirring under air for 3 h, the resulting mixture was extracted with AcOEt (300 mL × 3). The combined organic layer was washed with H_2O (200 mL × 2) and brine (100 mL × 2), dried over anhydrous Na_2SO_4, filtered, and evaporated to give colorless solid (1.1 g). The crude product was dissolved in hot MeOH (70 mL) and filtrated. The filtrate was evapolated to afford the desired product **5** as a colorless solid (1.1 g, 7.0 mmol, 91 %). ^{1}H NMR (400 MHz, $CDCl_3$/TMS) : δ = 7.56 (s, 2H), 2.38 (s, 6H).

Synthesis of 6. This reaction was performed under Ar atmosphere. 1,2-dicyano-4,5-dimethylbenzene **5** (2.11 g, 13.5 mmol) was dissolved in ethylene glycol (48 mL) in a 100 mL schlenk flask. $Fe(CO)_5$ (1.0 mL, 7.41 mmol) was added slowly at 180 °C. The mixture was stirred for 1 h at the bath temperature of 200 °C, and then, cooled to room temperature. After the mixture was diluted with 50 mL of H_2O, the resulting precipitate was filtered, washed with H_2O (300 mL) and MeOH (300 mL) successively to afford the desired compound **6** as a dark green solid (1.11 g, 1.63 mmol, 48%). This compound was used for the next reaction without further purification. MALDI-TOF MS : *m/z* = 680.21: calcd for $C_{40}H_{32}FeN_8$ ([**6**]$^{+}$) found: 680.26.

Synthesis of 4^{+}·I^{-}. **6** (162 mg, 238 μmol), NaN_3 (185 mg, 2.85 mmol), and 1-chloronaphthalene (2.7 mL) were placed in a 50 mL flask. The mixture was refluxed under air at the bath temperature of 190 °C for 20 h. After the reaction mixture was diluted with hexane (50 mL), the precipitate was collected by suction filtration, washed with hexane (100 mL) and H_2O (300 mL), successively, dried under vacuum to give blackish green solid (160 mg). The crude product was dissolved in pyridine (500 mL). After iodine (138 mg, 1.09 mmol as I) was added, the resulting solution was stirred for 37 h at room temperature, followed by evaporation of the volatile compounds. The residue was washed with Et_2O (500 mL × 3) to remove the remaining iodine, and then, dried under reduced pressure to give dark green solid. The obtained solid was dissolved in pyridine (500 mL) and the undissolved compound was removed by filtration. H_2O (1.5 L) was added in the filtrate to give dark green precipitate (98 mg). The precipitate was dissolved in a mixture of pyridine and $CHCl_3$ (1 : 1 (v/v), 30 mL) and the undissolved solid was removed by filtration. After the filtrate was evaporated, the residue was purified by silica gel column chromatography (4.5 cmϕ × 8.0 cm, hexane : $CHCl_3$: pyridine = 1 : 2 : 1) to give the desired compound **4**$^{+}$·I^{-} as a bluish green solid (26 mg, 17 μmol, 14%). ^{1}H-NMR (400 MHz, pyridine-d_5/TMS) : δ = 9.21 (s, 16H), 3.23 (s, 48H). MALDI-TOF MS : *m/z* =1374.42 : calcd for $C_{80}H_{64}Fe_2N_{17}$ ([**4**]$^{+}$) found: 1374.48. Anal. calcd for $C_{120}H_{104}Fe_2IN_{25}$ (**4**$^{+}$·I^{-}·8Pyridine): C; 67.51, H; 4.91, N; 16.40, found: C; 67.62, H; 4.63, N; 16.28 (0.28% error).

Preparation of silica-supported catalyst (**4**$^{+}$·I^{-}/SiO_2)**.** **4**$^{+}$·I^{-} (9.6 mg, 4.7 μmol) was dissolved in 25 mL of mixture of pyridine and $CHCl_3$ (1 : 1 (v/v)). After the addition of silica gel (830 mg) to the solution, the mixture was sonicated for 15 min. Solvent was evaporated. Pyridine (5 mL) and $CHCl_3$ (5 mL) was added to the residue, followed by sonication for 10 seconds. After solvent was evaporated, the residue was dried under vacuum at 60 °C for 13 h. The catalyst was suspended in an aqueous TFA (TFA 5.0 mL + H_2O 50 mL). The mixture was sonicated for 10 min and then the solid was filtered.

This TFA wash procedure was repeated twice. Finally, the resulting solid was washed with H_2O (700 mL) and dried under vacuum at 60 °C for 12 h. The silica-supported catalyst was obtained quantitatively. Silica-supported catalyst of $\mathbf{1}^{+}\cdot I^{-}$ ($\mathbf{1}^{+}\cdot I^{-}/SiO_2$) was prepared in a similar manner.

Cyclic voltammogram of $\mathbf{4}^{+}\cdot I^{-}$. Cyclic voltammograms were measured with a BAS Electrochemical Analyzer Model 750Ds at room temperature in pyridine solutions containing 100 mM $TBAPF_6$ in a standard one-component cell under an N_2 atmosphere equipped with a 3 mm-O.D. glassy carbon disk working electrode, platinum wire counter electrode, and Ag/AgCl reference electrode. All solutions were deoxygenated by N_2 bubbling for at least 20 min. Obtained $E°'$ vs. Ag/AgCl were converted to those *vs.* Fc/Fc^{+} based on measured redox potential of ferrocene. Tetrabutylammonium hexafluorophosphate ($TBAPF_6$) was recrystallized from 95% EtOH and dried under vacuum overnight at 100 °C.

Methane oxidation reactions. Methane oxidation reaction was performed in a stainless-steel autoclave with a glass tube. A mixture containing the catalyst on SiO_2 (30 mg, 55 μM as $\mathbf{4}^{+}\cdot I^{-}$ or $\mathbf{1}^{+}\cdot I^{-}$), 35% aqueous H_2O_2 (50 μL, 189 mM), and TFA (12 μL, 51 mM) in H_2O (3.0 mL) was heated at 60 °C under 1.0 MPa of methane for 4–16 h with continuous stirring (900 rpm). After the autoclave was opened, the reaction mixture was filtrated through a disposable membrane filter. The filtrate was analyzed by GC-MS (system: Agilent 7890A equipped with JEOL JMS-T100GCV, detection: EI, column: Agilent DB-WAX UI, external standard: isovaleric acid (5 mM), temperature conditions: initial: 70 °C to 220 °C (10 °C/min) – hold (5 min)). The yields of methanol and formic acid were determined based on the results of GC-MS. The yield of formaldehyde was examined using the method reported by Yu et al as reported in our previous paper.[17,19,25]

Conflicts of interest

There are no conflicts to declare.

Acknowledgements

This work was financially supported by a JSPS KAKENHI Grant-in-Aid for Scientific Research (B) (Number 19H02787), JST PRESTO (Number JK114b) for YY, and a JSPS KAKENHI Grant-in-Aid for Scientific Research (A) (Number 19H00902) to KT.

Notes and references

1 P. C. Bruijnincx and B. M. Weckhuysen, *Angew. Chem. Int. Ed.*, 2013, **52**, 11980-11987.

2 Z. Guo, B. Liu, Q. Zhang, W. Deng, Y. Wang, Y. Yang, *Chem. Soc. Rev.*, 2014, **43**, 3480–3524.

3 S. J. Blansby and G. B. Ellinton, *Acc. Chem. Res.*, 2003, **36**, 255.

4 M. Ravi, M. Ranocchiari, J. A. van Bokhoven, *Angew. Chem. Int. Ed.*, 2017, **56**, 16464–16483.

5 Z. Liang, T. Li, M. Kim, A. Asthagiri, J. F. Weaver, *Science*, 2017, **356**, 299–303.

6 B. E. R. Snyder, P. Vanelderen, M. L. Bols, S. D. Hallaert, L. H. Böttger, L. Ungur, K. Pierloot, R. A. Schoonheydt, B. F. Sels, E. I. Solomon, *Nature*, 2016, **536**, 317–321.

7 J. Shan, M. Li, L. F. Allard, S. Lee, M. Flytzani-Stephanopoulos, *Nature*, 2017, **551**, 605–608.

8 V. L. Sushkevich, D. Palagin, M. Ranocchiari, J. A. van Bokhoven, *Science,* 2017, **356**, 523–527.

9 C. Hammond, M. M. Forde, M. H. Ab Rahim, A. Thetford, Q. He, R. L. Jenkins, N. Dimitratos, J. A. Lopez-Sanchez, N. F. Dummer, D. M. Murphy, A. F. Carley, S. H. Taylor, D. J. Willock, E. E. Stangland, J. Kang, H. Hagen, C. J. Kiely, G. J. Hutchings, *Angew. Chem. Int. Ed.*, 2012, **51**, 5129–5133.

10 A. Hu, J.-J. Guo, H. Pan, Z. Zuo, *Science*, 2018, **361**, 668–672.

11 K. Ohkubo, K. Hirose, *Angew. Chem. Int. Ed.*, 2018, **57**, 2126–2129.

12 K. T. Smith, S. Berritt, M. González-Moreiras, S. Ahn, M. R. Smith III, M.-H. Baik, D. J. Mindiola, *Science*, 2016, **351**, 1424–1427.

13 P. Afanasiev, A. B. Sorokin, *Acc. Chem. Res.*, 2016, **49**, 583–593.

14 A. B. Sorokin, E. V. Kudrik, D. Bouchu, *Chem. Commun.*, 2008, 2562–2564.

15 E. V. Kudrik, P. Afanasiev, L. X. Alvarez, P. Dubourdeaux, M. Clémancey, J.-M. Latour, G. Blondin, D. Bouchu, F. Albrieux, S. E. Nefedov, A. B. Sorokin, *Nature Chem.*, 2012, **4**, 1024–1029.

16 Ü. ís¸ci, A. S. Faponle, P. Afanasiev, F. Albrieux, V. Briois, V. Ahsen, F. Dumoulin, A. B. Sorokin, S. P. de Visser, *Chem. Sci.*, 2015, **6**, 5063–5075.

17 Y. Yamada, K. Morita, N. Mihara, K. Igawa, K. Tomooka, K. Tanaka, *New J. Chem*., 2019, **43**, 11477–11482.

18 S. I. Chan, Y.-J. Lu, P. Nagababu, S. Maji, M.-C. Hung, M. M. Lee, I-J. Hsu, P. D. Minh, J. C.-H. Lai, K. Y. Ng, S. Ramalingam, S. S.-F. Yu, M. K. Chan, Angew. Chem. Int. Ed., 2013, 52, 3731–3735.

19 S. Sirajuddin, A. C. Rosenzweig, *Biochemistry*, 2015, **54**, 2283–2294.

20 V. C.-C. Wang, S, Maji, P. P.-Y. Chen, H. K. Lee, S. S.-F. Yu, S. L. Chan, *Chem. Rev.*, 2017, **117**, 8574–8621.

21 E. Y. Tshuva, S. J. Lippard, *Chem. Rev.*, 2004, **104**, 987–1012.

22 X. Shan, L. Que Jr., *J. Inorg. Biochem.*, 2006, **100**, 421-433.

23 W. Nam, *Acc. Chem. Res.*, 2007, **40**, 522–531.

24 A. R. McDonald, L. Que Jr., *Coord. Chem. Rev.*, 2013, **257**, 414–428.

25 W. Nam, *Acc. Chem. Res.*, 2015, **48**, 2415–2423.

26 W. Nam, H. J. Han, S.-Y. Oh, Y. J. Lee, M.-H. Choi, S.-Y. Han, C. Kim, S. K. Woo, W. Shin, *J. Am. Chem. Soc.*, 2000, **122**, 8677–8684.

27 S. Yokota, H. Fujii, *J. Am. Chem. Soc.*, 2018, **140**, 5127–5137.

28 K. Yamaguchi, Y. Watanabe, I. Morishima, *Inorg. Chem.*, 1992, **31**, 156–157.

29 Ü. ís¸ci,P. Afanasiev, J.-M. M. Millet, E. V. Kudrik, V. Ahsen, A. B. Sorokin, *Dalton Trans.*, 2009,7410–7420.

30 P. Afanasiev, D. Bouchu, E. V. Kudrik, J.-M. M. Millet, A. B. Sorokin, *Dalton Trans.*, 2009, 9828–9836.

31 P. Afanasiev, E. V. Kudrik, J.-M. M. Millet, D. Bouchu, A. B. Sorokin, *Dalton Trans.*, 2011, **40**, 701–710.
32 C. Colomban, E. V. Kudrik, V. Briois, J. C. Shwarbrick, A. B. Sorokin, P. Afanasiev, *Inorg. Chem.*, 2014, **53**, 11517–11530.
33 R. Silaghi-Dumitrescu, S. V. Makarov, M.-M. Uta, I. A. Dereven'kov, P. A. Stuzhin, New J. Chem., 2011, 35, 1140–1145.
34 M. G. Quesne, D. Senthilnathan, D. Singh, D. Kumar, P. Maldivi, A. B. Sorokin, S. P. de Visser, *ACS Catal.*, 2016, **6**, 2230–2243.
35 M. Ansari, N. Vyas, A. Ansari, G. Rajaraman, *Dalton Trans.*, 2015, **44**, 15232–15243.
36 Q. M. Phung, K. Pierloot, *Chem. Eur. J.*, 2009, **25**, 12491–12496.
37 Y. Yamada, J. Kura, Y. Toyoda, K. Tanaka, *New. J. Chem.*, 2020, **44**, 19179-19183.
38 C. Hansch, A. Leo, R. W. Taft, *Chem. Rev.*, 1991, **91**, 165–195.
39 Y. Yamada, T. Sugiura, K. Morita, H. Ariga-Miwa, K. Tanaka, *Inorg. Chim. Acta*., 2019, **489**, 160-163.
40 V. L. Goedken, C. Ercolani, *J. Chem. Soc., Chem. Commun.*, 1984, 378–379.
41 L. A. Bottomley, B. B. Garrett, *Inorg. Chem.,* 1982, **21**, 1260-1263.
42 K. M. Kadish, R. K. Rhodes, L. A. Bottomley, H. M. Goff, *Inorg. Chem.,* 1981, **20**, 3195-3200
43 M. Li, M. Shang, N. Ehlinger, C. E. Schulz, R. W. Scheidt, *Inorg. Chem.,* 2000, **39**, 580-583.
44 N. Mihara, Y. Yamada, H. Takaya, Y. Kitagawa, K. Igawa, K. Tomooka, H. Fujii, K. Tanaka, *Chem. Eur. J*., 2019, **25**, 3369–3375.
45 L. A. Bottomley, J.-N. Gorce, V. L. Goedken, C. Ercolani, *Inorg. Chem.*, 1985, **24**, 3733–3737.
46 T. C. Bruice, M. F. Zipplies, W. A. Lee, *Proc. Natl. Acad. Sci. USA*, 1986, **83**, 4646–4649.
47 D. R. Weinberg, C. J. Gagliardi, J. F. Hull, C. F. Murphy, C. A. Kent, B. C. Westlake, A. Paul, D. H. Ess, D. G. McCafferty, T. J. Meyer, *Chem. Rev.*, 2012, **112**, 4016–4019.
48 J. E. M. N. Klein, G. Knizia, *Angew. Chem. Int. Ed.*, 2018, **57**, 11913–11917.